HHS Public Access

Author manuscript

J Biomed Mater Res A. Author manuscript; available in PMC 2022 December 18.

Published in final edited form as:

J Biomed Mater Res A. 2021 July ; 109(7): 1065–1079. doi:10.1002/jbm.a.37097.

Advancing Continuous Subcutaneous Insulin Infusion *in vivo*: New Insights into Tissue Challenges

Shereen Kesserwan, M.S.[1], **Adam Mulka, B. S.**[1], **Roshanak Sharafieh, Ph.D.**[2], **Yi Qiao, M.D.**[2], **Rong Wu, Ph.D., M.S.**[3], **Don Kreutzer, Ph.D.**[2], **Ulrike Klueh, Ph.D.**[1,2,4]

[1]Integrative Biosciences Center (IBio), Department of Biomedical Engineering, Wayne State University, Detroit, MI 48202

[2]UConn Health, School of Medicine, Department of Surgery

[3]Connecticut Convergence Institute for Translation in Regenerative Engineering, Farmington, CT 06030

Abstract

Continuous Subcutaneous Insulin Infusion (CSII) is superior to conventional insulin therapy as it improves glycemic control thus reducing the probability of diabetic complications. Notwithstanding CSII's benefits, insulin dependent diabetic patients rarely achieve optimal glucose control. Moreover, CSII is only FDA approved for 3 days and often fails prematurely for reasons that have not been fully elucidated. We hypothesize that phenolic compounds, such as m-cresol and phenol, which are present in all commercial insulin formulations are responsible for the tissue reaction occurring at the insulin infusion site. This hypothesis was examined with *in vitro* cell cultures and a mouse air-pouch model to determine cellular and tissue reactions following infusions with saline, phenolic compounds, (i.e. commercial diluent), and insulin. We demonstrated that diluent and insulin were cytotoxic to cells in culture at sub-clinical concentrations (e.g. >1:10 of commercial insulin). Air pouch studies demonstrated that infusion of either diluted insulin or diluent itself induced 3 to 5-fold level of recruited leukocytes as compared to saline. At both 3- and 7-days post-infusion, these were predominantly neutrophils and macrophages. We conclude that phenolic compounds in commercial insulin preparations are cell and tissue toxic, which contributes to the failure of effective insulin infusion therapy.

Keywords

phenolic compounds; diabetes; phenol and m-cresol; inflammation; insulin therapy; continuous subcutaneous insulin infusion; murine air pouch model

[4]**Corresponding Author:** Ulrike Klueh Ph. D., klueh@wayne.edu, Tel.: (313) 577-4790.

Author Disclosure Statement

Ulrike Klueh, Ph.D. and Don Kreutzer, PhD are co-founders and co-owners of the small business Cell and Molecular Tissue Engineering, LLC, Avon CT. No other potential conflicts of interest relevant to this article are present.

Introduction

Technological advances in continuous glucose monitoring (CGM) have improved diabetes care over the past three decades [1]. Transdermal CGM systems are currently FDA approved for a 14-day duration [2]. In contrast, insulin infusion systems, which are a vital component of any artificial pancreas, often fail before the FDA approved three-day duration [3–5]. This reduced lifespan of these continuous subcutaneous insulin infusion (CSII) sets hinders the development of an artificial pancreas, which requires that both CGM and CSII have similar functional lifespans. Furthermore, insulin infusion remains one of the least studied, but most critical element of an integrated artificial pancreas system [6].

The typical *in vivo* functional time for the two to three-day CSII has been attributed to tissue effects such as skin irritation, lipohypertrophy, and altered insulin pharmacokinetics (PK), which ultimately leads to a loss of glycemic control [7–10]. Recently, it was reported that device site-specific inflammation may be responsible for this short functional lifespan [11]. Specifically, Weber *et al.* demonstrated that insulin additives, such as phenol and m-cresol, induce expression of inflammatory cytokines, including the chemokine MCP-1 *in vitro* [11]. Subsequently, Hauzenberger *et. al.* reported that inflammation might function as a mechanical barrier to insulin flow in a swine model [12]. In addition, Teflon versus steel catheter materials were compared in order to determine the specific effects of material-induced inflammation at CSII sites, but no significant differences were observed [13–16].

Currently, only rapid or short-acting insulin formulations are utilized in infusion pumps of which four are available in the domestic market and five are available in Europe (Table 1). All insulin infusion formulations contain phenolic compounds, mainly meta-cresol (m-cresol) and phenol, in significant concentrations (2.3–3.2 mg/ml) (Table 1). Cresols are methylated phenols that are colorless aromatic organic compounds, which occur in three isomers; o-cresol, m-cresol, and p-cresol depending on the location of the methyl group [17]. Cresols have a very distinct odor and are widely used as synthetic intermediates to polymers, pesticides, paint, and pharmaceuticals [18]. The phenolic compounds, such as phenol and m-cresol, in insulin formulations provide insulin protein stability, sterility and ensure a prolonged shelf-life [6, 10, 19, 20]. Nevertheless, these compounds are believed to manifest tissue toxicity as they have shown to induce expression of inflammatory cytokines *in vitro* [11]. Thus, identifying and mitigating the mechanisms by which an insulin formulation and specifically its phenolic compounds induce tissue toxicity would overcome an important obstacle to increasing the lifespan of insulin infusion sets including artificial pancreas systems. Therefore, the aim of the present study is to investigate the cell and tissue toxicity as well as tissue reactions to phenolic compounds *in vitro* and *in vivo*. Specifically, we focused on sterile diluent, provided by Eli Lilly and Company, as our phenolic compound. Diluent has a combined m-cresol and phenol concentration of 2.25 mg/ml (Table 1). We hypothesized that phenolic compounds, key components of commercial insulin formulations, are both cell and tissue toxic. We also hypothesized that these reagents, either when injected or infused into the subcutaneous tissue, would trigger inflammation. To evaluate the impact of phenolic compounds on cells, we evaluated both Humalog insulin and diluent on primary and tissue culture cell lines to demonstrate that phenolic compounds are toxic *in vitro*. In order to gain an understanding of the underlying

mediators and mechanisms that drive the tissue reactions at the site of phenolic compound infusion, we developed a modified murine air pouch model that allows for the collection of cell and fluid contents at the catheter infusion sites for subsequent analyses. Using this mouse model, we demonstrated that phenolic compounds induce an influx of leukocytes at infusion sites in non-diabetic and chemically induced diabetic mice. This model could provide a useful method to develop agents and infusion devices that can prevent and/or overcome destructive tissue reactions that limit insulin effectiveness. These studies support the hypothesis that phenolic compounds induce a profound acute inflammatory response, such that methodologies that would attenuate the inflammatory response could potentially extend the useful lifespan of CSII devices.

Materials and methods

Cell lines, cell culture, and differentiation

Mouse Macrophage cells (RAW 264.7), and Embryonic Fibroblasts (3T3-L1) were purchased from ATCC (Manassas, VA) and cultured according to suppliers' instructions. Bone marrow derived mast cells (BMMC) were isolated from bones of C57BL/6J mice as previously described by Klueh *et. al* [21]. Human Peripheral Blood Mononuclear Cells (PBMC) were isolated in house. Briefly, heparinized blood was obtained from healthy donors and processed for PBMC isolation following the manufacturer's Histopaque-1077 protocol (Sigma-Aldrich, St. Louis, MO). The heparinized blood was diluted at a ratio of 1:1 with Histopaque-1077 and gently mixed prior to centrifugation at 400 x g for 30 minutes at room temperature. Next, the upper layer was carefully removed and discarded without disturbing the PBMC containing middle layer. PBMCs were transferred to a clean tube and gently suspended using 3x the volume of PBS. Cells were centrifuged at 250 x g for 10 minutes prior to plating them in a 48-well tissue culture plate for use in the cytotoxicity assay.

Removal of Phenolic Compounds from Commercial Insulin

Apidra (Sanofi, Bridgewater, NJ), Humalog (Eli Lilly & Co., Indianapolis, IN), and Novolog (Novo Nordisk, Plainsboro Township, NJ) purchased from a pharmacy were passed through spin Zeba desalting columns (Thermo Fisher Scientific, Waltham, MA) to remove phenolic compounds [22]. The column was placed in a 1.5–2.0mL collection tube and centrifuged at 1500 × g for 1 minute to remove storage solution. Next, 300μL of PBS was passed through the column by centrifugation at 1500 × g for 1 minute. After washing the resin 3 times, the column was placed in a new collection tube and commercial insulin was applied to the top of the compact resin bed. Insulin was eluted by centrifugation at 1500 × g for 2 minutes and collected. A standard protein assay (Thermo Fisher Scientific, Waltham, MA) was performed on the post-column eluates to confirm retrieval of insulin protein following removal of phenolic compounds.

MTT cytotoxicity assay

MTT assay is widely used to show loss of cellular metabolic activity (ATCC bioproducts, Manassas, VA). Cells undergoing analysis via the cytotoxicity assay were plated in a 48-well plate with $2.5x10^5$ cells/well. These cells were incubated overnight in 250μl of the growth

media required for each individual cell line. Mouse cell lines and PBMCs were exposed to saline, sterile diluent (Eli Lilly and Company, Indianapolis, IN) and Humalog (Eli Lilly and Company, Indianapolis, IN) at a serial dilution of 1:3 for 1 and 3-days. PMBCs were also exposed to Apidra (Sanofi, Bridgewater, NJ), Humalog (Eli Lilly & Co., Indianapolis, IN), and Novolog (Novo Nordisk, Plainsboro Township, NJ) with and without phenolic compounds at a serial diluent of 1:3 for 1-day. Following an incubation period of 3 days for PBMC and 1- and 3-days for mouse cell lines, 30μl of MTT reagent was added to each well and plates were incubated for 1 hour at 37°C until visibility of purple precipitate. Next, all supernatants were discarded and 300μl DMSO was added, mixed well, and 100μl samples were transferred to a 96-well plate in duplicates. Absorbance was read at 570 nm for analysis.

Mice

Outbred Hsd:ICR-CD-1 (CD-1) mice were purchased from Envigo (Somerset, NJ) or maintained at in-house facilities. Mice were maintained under temperature- and light-controlled conditions (20–24°C, 12-hr light-dark cycle) receiving food and water ad libitium. Mice used in these studies had an average weight between 30 – 40 g. All studies were conducted with approval from the institutional animal care and use committee (IACUC) at Wayne State University.

Streptozotocin induction

Diabetes was induced following the protocol developed by Wu *et. al* [23]. As female mice are not susceptible to streptozotocin (STZ) treatment, only STZ induced diabetic male mice are used in chemical induced diabetes studies [23]. As such, only male mice received daily intraperitoneal (i. p.) injections of STZ (50 mg STZ/kg body weight) for a period of 5 days (Sigma-Aldrich, St. Louis, MO). STZ was prepared by dissolving 50 mg STZ in 100 mM sodium citrate buffer (pH=4.5) and immediately injected following the preparation. Blood glucose levels were monitored at least twice weekly following STZ treatment using a Bayer Contour Next EZ Meter (Ascensia Diabetes Care, Parsippany, NJ). Mice with a blood glucose level above 250 mg/dL for two sequential blood glucose tests were designated as diabetic and subsequently used for the infusion studies.

Murine air pouch model

The classic murine air pouch model (Figure 3) was adapted in an effort to evaluate the tissue response to injected agents [24–26]. Briefly, 3 mL of filtered air (Millipore, 0.22 μm) was injected subcutaneously (s. c.) into the shaved dorsal area of CD-1 mice creating a sustained compartment (pouch) (Figure 3B). Subsequent infusion studies were initiated 1- and 3-day following air pouch initiation (Figure 3C). At 3- or 7-days following initiation of infusion, the mouse was sacrificed, and the air pouch was lavaged with a total volume of 10 ml 0.9% w/v saline (Baxter, Deerfield, IL) with 1mM EDTA (Sigma-Aldrich, St. Louis, MO). Resulting contents of the air pouch were analyzed for total leukocyte cell number counts using the TC20 automated cell counter (Bio-Rad, Hercules, CA) and leukocyte subpopulations using Fluorescent Activated Cell Sorter (FACS) for cytometry analysis (Figure 3D). Qualitative histopathologic tissue evaluation of the air pouch wall

tissue was conducted at 3- and 7-day post-initiation of the infusion studies using H&E, Masons Trichrome (collagen) and macrophages (F4/80 immunohistochemistry) (Figure 3D).

Infusion catheter implantation in the mouse

Infusion set cannulas were implanted into the air pouch of anesthetized mice (Animas Inset 30 Infusion System, ADW Diabetes, Pompano Beach, FL) (Figure 3C). Next, the catheter was secured to the mouse skin with the adhesive catheter patch and adhered to the skin with an additional nylon mesh to prevent the device from dislodging by the mouse (Figure 3C). The nylon mesh was glued to the mouse skin using liquid bandage. Mice were housed individually to prevent dislodging of the device from aggressive behavior between mice (Figure 3E).

Continuous infusion into the murine air pouch

Continuous infusion at a rate of 50μL/hour for either 3- or 7-days was initiated immediately following catheter insertion. Non-diabetic mice were infused with saline as the control solution or sterile diluent (Eli Lilly & Co., Indianapolis, IN) as the choice for phenolic compound solution. Sterile diluent has a combined phenolic compound of 2.25 mg/ml m-cresol and phenol, 1.6 mg/ml and 0.65, respectively (Table 1). Chemically induced diabetic mice received periodic infusion of 1U Humalog U100 (Eli Lilly & Co., Indianapolis, IN) diluted 1:100 in sterile diluent. In order to avoid hypoglycemic events in Humalog treated mice, Humalog infusion was periodically changed to sterile diluent only. This infusion procedure for diabetic mice ensured that an equal infusion volume was maintained between different treatment groups. Blood glucose of the diabetic mice was sporadically evaluated using a Bayer Contour Next meter (Whippany, NJ). Standard infusion-only pumps were obtained from Harvard Apparatus (Holliston, MA), and 1000 series gastight infusion syringes were obtained from Fisher Scientific (Waltham, MA) (Figure 1D).

Leukocyte isolation from mouse air pouch

At 3- or 7-days post-infusion, mice were euthanized, and the air pouch was lavaged by injecting a total volume of 10 mL of 0.9% w/v saline (Baxter, Deerfield, IL) with 1mM EDTA (Sigma-Aldrich, St. Louis, MO). To ensure collecting the maximum cell volume, the mouse air pouch was gently massaged while extracting the injected saline volume. Next, the collected cell fluid was centrifuged at 1000 rpm for 5 minutes. The cell pellet was mixed by gently pipetting up and down and washed twice with 10 mL FACS buffer (2% fetal bovine serum (Atlanta Biologicals, Flowery Branch, GA) in phosphate buffer saline (PBS) (Fisher Scientific, Waltham, MA)) prior to cell counting using a TC20 Automated Cell Counter (Bio-Rad, Hercules, CA). Cells were re-suspended to a density of $>1x10^6$ cells in 100 μL FACS buffer.

Leukocyte Flow Cytometry (FACS) Analysis

For identification of the leukocyte population derived from the air pouch, single cell suspensions were stained with fluorescent labeled antibodies to detect myeloid cells ($CD45^+CD11b^+$), neutrophils ($CD45^+CD11b^+Ly6G^+$), macrophages ($CD45^+$ $CD11b^+$ $Ly6G^-$; $Ly6G^{low}$), monocytes ($CD45^+$ $CD11b^+$ $Ly6G^-$; $Ly6G^{high}$), and lymphocytes (SSC-

$A^{-;}$ $CD45^{high}$) [27]. Leukocyte cell populations were incubated with 0.5 μL Fc-blocking agent (anti-mouse CD 16/32, Biolegend, San Diego, CA) for 10 minutes at room temperature prior to the addition of the multi-color antibody panel. Fluorescent minus one (FMO) controls were used to differentiate between positively and negatively stained populations. Compensation was performed using BD Comp Beads (BD Biosciences, San Jose, CA) to create single-color controls of each antibody. All antibodies were obtained from Biolegend (San Diego, CA), unless otherwise stated. FACS analysis was performed on a BD LSR II utilizing the services of the microscopy, imaging, and cytometry core laboratory (MICR), at Wayne State University, Detroit, MI, and data was analyzed with FlowJo software (FlowJo, LLC).

Histological Evaluation

In order to evaluate tissue responses to the respected air pouch infusions, qualitative histopathologic evaluation was performed on mouse tissue samples at 3- and 7-days post-infusion. Mice were euthanized, the air pouch was lavaged, removed and fixed in 10% buffered formalin (VWR, Radnor, PA) for 24 hours, followed by standard tissue preparatory steps, paraffin embedding, and sectioning. Tissue samples were cut into 5 μm sections and stained using standard Hematoxylin and Eosin stain (H&E) and Masson's Trichrome stain. Tissue samples were evaluated using a Nikon microscope and imaging system. Histopathological evaluation included the extent of inflammation comprising leukocyte populations, disruption of tissue architecture, and fibrosis in the mouse air pouch. The extent of inflammation and the degree of inflammatory cell infiltration at air pouch site was reported for each injected test agent.

Immunohistochemical staining of Macrophages using F4/80

To confirm the presence of macrophages in the air pouch tissue sections, we utilized a mouse macrophage-specific antibody, designated anti-mouse F4/80 (Fisher Scientific, catalog # MF48000, Waltham, MA). Mouse IgG was used as a negative control.

Statistical Analysis

All analyses were conducted using SAS version 9.4 (SAS, Inc., Cary, NC). Two-sided testing was employed to assess for statistical significance at an alpha of 0.05. For normative data comparing two groups, a two-sample unpaired t-test was employed. For multiple group comparisons, a one-way or two-way ANOVA was utilized to assess for a significant difference between these groups as a 95% confidence interval. For those tests achieving statistical significance, pairwise comparisons underwent an additional Tukey adjustment. Following FACS staining and analysis of the cell populations, all cell numbers were visualized using boxplots, which were generated by R 3.6.2 software. Line graphs related to in vitro cell studies were generated using GraphPad Prism 8.4.3 software.

Results

Cytotoxicity of commercial insulin to human PBMC in vitro

We first demonstrated the cytotoxic effects of insulin excipients *in vitro* on Human PBMC (Figure 1). Insulin formulations Humalog, Apidra and Novolog, which contain >3mg/mL

m-cresol/phenol were incubated with cells for 1 day. Formulations were diluted to determine dose response. Figure 1 indicates that cytotoxic effects are at a concentration of 0.5mg/mL of commercial insulin (1:6 dilution) for all tested insulin formulations. When m-cresol and/or phenol were removed by Zeba spin filter columns, designated as pure, these cytotoxic effects were no longer observed, showing statistical significance ($p<0.05$) between normal formulations and their purified versions (Supplementary Table S1). A protein assay performed following removal of excipients indicated a 99% retrieval of insulin protein (data not shown). Given that the magnitude of cytotoxicity was similar for Humalog, Apidra and Novolog, Humalog was randomly selected for the remaining studies.

Cytotoxicity of Humalog and sterile diluent to mouse cell lines in vitro

Initial cytotoxicity studies were then expanded into mouse cell lines to determine which cell types are susceptible to m-cresol and phenol cytotoxicity. *In vitro* experiments shown in Figure 2 demonstrate that different mouse cell lines all manifested similar reactivity to m-cresol and phenol containing insulin formulations, which emphasizes the non-specific cytotoxicity of these two compounds. A two-way ANOVA test (Supplementary Table S2) indicated statistical significance for both Insulin and Diluent treated cells when compared to Saline at dilutions between 1:3 and 1:12 in all cell studies, except for 1-day 3T3-L1 Fibroblasts ($p<0.05$).

A 1:12 dilution equates to an m-cresol concentration of 0.27 mg/ml in insulin samples and an m-cresol/phenol concentration of 0.13 mg/ml in diluent samples. One- and three-day data sets for each respective cell line demonstrate minimal changes in cell viability implying that viability is diminished within the first 24 hours of exposure (Figure 2).

Total Cell Count [TCC] and Cell Type [CT] analysis of lavage fluids following saline or diluent infusion into the air pouch of non-diabetic CD-1 mice for 3-days (3D) and 7-days (7D)

The tissue toxicity of insulin diluents in non-diabetic mice was determined by continuously infusing saline (S) or diluent (D) into the mouse air pouch at 50 μl/hr for either 3 days (3D) or 7 days (7D). As depicted in Figure 4 and Table 2, the total leukocyte count by FACS analysis following diluent infusion demonstrated a significant increase in cellular response at both 3D and 7D when compared to the saline infusion control ($p<0.01$ and $p<0.001$ respectively, Table 2B). A cellular subtype analysis of neutrophils (Figure 5A), monocyte/macrophages (Figure 5B) and lymphocytes (Figure 5C) is depicted in Figure 5. Neutrophils did not significantly increase between these two states in the control mice at 3D, whereas significantly more neutrophils were noted in the diluent infused group at 7D ($p<0.01$, Table 3B). Monocyte/macrophage analysis demonstrated significantly greater numbers in the diluent-treated control mice at both 3D and 7D ($p<0.01$ and $p<0.001$, respectively, Table 4B). Lymphocyte analysis demonstrated a significant increase in diluent treated mice at 3D ($p<0.01$), but not at 7D (Table 5B).

TCC and CT of lavage fluids following infusion of saline, diluent, or insulin into the air pouch of STZ-induced diabetic CD-1 mice for 3D and 7D

Three infusion treatments were compared in the STZ-induced diabetic CD-1 mice: saline (S), diluent (D) and insulin with diluent (I). There were significantly fewer cells in the saline infused mice, as compared to the other two states at both 3D and 7D ($p<0.001$ and $p<0.05$, respectively, Table 2C). However, there were no significant differences between the D, and I infused mice at either 3D or 7D (Table 2C). Figure 5 depicts the cellular subgroup analysis for these three states. A one-way ANOVA test on the 3D infusions demonstrated that there were significantly fewer neutrophils in the saline infused STZ-induced diabetic mice when compared to either the D or I infused mice ($p<0.02$, Table 3C). A Tukey's post-hoc analysis revealed a statistically significant increase in the diluent treated group when compared to the saline infused group ($p<0.02$, Table 3C). This same analysis demonstrated that there was a trend towards a greater number of neutrophils in the insulin infusion group as compared to the saline infused group, but this did not reach statistical significance (Table 3C). In contrast, no significant differences in neutrophils were observed between any of these groups for 7D. Monocyte/macrophage data demonstrated a significant difference between these three states at both 3D and 7D ($p<0.001$ and $p<0.05$ respectively, Table 4C). A post-hoc Tukey analysis revealed a significant difference at 3D between S and D as well as S and I ($p<0.01$ and $p<0.001$ respectively, Table 4C), whereas there was no significant difference detected between the D and I groups (Table 4C). The Tukey post-hoc analysis for 7D infusion demonstrated a similar trend as the 3D, but this did not reach statistical significance at a 95% confidence interval between S and D or S and I (Table 4C). With respect to the lymphocytes, a significant difference between these three states was detected at 3D, but not at 7D ($p<0.02$, Table 5C). Post-hoc analysis only demonstrated significantly fewer lymphocytes between the I and S groups at 3D ($p<0.02$, Table 5C).

Intragroup Comparison Analysis

A comparison was also conducted between 3D and 7D infusion with respect to cellular subtypes. A significant difference in neutrophil numbers between 3D and 7D was observed only for saline infused mice (Table 3D). Similarly, no significant differences were noted in the number of lymphocytes between 3D and 7D following both S and D infusions (Table 5D). In contrast, significantly more monocytes/macrophages were noted in the diluent treated control mice on day 3 than on day 7 ($p<0.02$, Table 4D). In the STZ-induced diabetic mice, no significant differences were noted for any cell subtype when day 3 was compared to day 7 following Bonferroni correction (Table 2–5D).

Tissue responses to reagent infused in air pouch of non-diabetic CD-1 mice

The tissue reaction induced by continuously infusing saline or diluent into the air pouch for either 3- or 7-days in non-diabetic CD-1 mice was then characterized. The air pouch tissue was evaluated using standard histopathology techniques (Figure 6). Histopathologic evaluation of the air pouch tissue demonstrated that diluent-alone induced more robust inflammation at 3 and 7-days post-infusion when compared to saline infusion.

Day 3 saline infusion in non-diabetic mice: Saline infused air pouch tissue displayed light scattering of inflammatory cells within the tissue associated with a more intense gathering of inflammatory cells at the tissue next to the air pouch (Figure 6A). These inflammatory cells included both neutrophils and macrophages. No detectable collagen deposition was seen in the saline infused air pouch tissue (Figure 6E). Analysis of macrophage distribution demonstrated a limited number of macrophages present at day 3 in the air pouch tissue. The limited macrophages present tended to be associated at the interface between the tissue and air pouch (Figure 6I).

Day 3 diluent infusion in non-diabetic mice: After 3 days of diluent infusion, a moderate scattering of inflammatory cells was observed in the tissue adjoining the air pouch. These inflammatory cells included both neutrophils and macrophages. Collagen deposition can be observed as blue bands within the air pouch tissue (Figure 6F). An appearance of extensive numbers of macrophages was seen both at the air pouch tissue interface associated with spreading into the adjacent tissue (Figure 6J).

Day 7 saline infusion in non-diabetic mice: Saline infused air pouch tissue displayed a paucity of inflammatory cells scattered within the tissue (Figure 6C). No detectable new collagen deposition was observed in the saline infused air pouch tissue (Figure 6G). Analysis of the macrophage distribution in the 7-day saline infused tissue demonstrated limited number of macrophages scattered in the air-pouch tissue on day 7 (Figure 6K). Overall, the tissue reactions after 7 days of saline infusion (Figure 6C, G, K) were minimal when compared to the 3-day saline infusion tissue reactions (Figure 6A, E, I). Thus, we infer that the initial tissue reaction induced by the saline infusion was likely the result of the initial cannula insertion and the associated acute tissue reaction.

Day 7 diluent infusion in non-diabetic mice: At 7-days post-diluent infusion, a significant inflammatory cell presence was observed including enhanced cellularity at the air pouch interface (Figure 6D). Further analysis indicated that macrophages were a significant percentage of the inflammatory cells present on day 7, including both tissue and interface regions of the air pouch tissue site (Figure 6L). Additionally, collagen deposition was present at the 7-day diluent infusion site (Figure 6H). This collagen deposition was likely a result of remodeling that was occurring at the air pouch tissue site.

Tissue responses to reagent infused in air pouch of diabetic CD-1 mice

In order to determine if diabetes affects the tissue reaction to saline, sterile diluent or diluted Humalog were infused continuously into the air pouch of the chemically- induced diabetic mice for a period of 3 to 7 days.

Day 3 saline infusion in diabetic mice: Saline-infused air pouch tissue displayed light scattering of inflammatory cells within the tissue, with a more intense gathering of inflammatory cells at the tissue next to the air pouch (Figure 7A). These inflammatory cells included both neutrophils and macrophages. Slight collagen deposition was noted in the saline infused air pouch tissue (Figure 7G). Analysis of macrophage distribution

demonstrated a limited macrophage presence post 3-day infusion, which tended to be associated at the interface between the tissue and air-pouch (Figure 7M).

Day 3 diluent infusion in diabetic mice: At day 3 of diluent infusion, a moderate scattering of inflammatory cells was seen in the tissue adjoining the air pouch (Figure 7B). These inflammatory cells included both neutrophils and macrophages. Collagen deposition appears as blue bands within the air pouch tissue (Figure 7H). In addition, substantial numbers of macrophages were observed spreading into the tissue adjacent to the air pouch (Figure 7N).

Day 3 insulin infusion in diabetic mice: At 3 days of insulin (with diluent) infusion in diabetic mice, there was significant inflammation observed at the air pouch tissue interface (Figure 7C). Additionally, inflammatory cells were spread throughout the air pouch tissue (Figure 7C). Of note, collagen deposition was also observed within the air pouch tissue (Figure 7I). Neutrophils and macrophages were noted within the air pouch interface and surrounding tissue (Figure 7C). The distribution of macrophages in the air pouch interface and surrounding tissue was confirmed using F4/80 immunohistochemistry (Figure 7O).

Day 7 saline infusion in diabetic mice: Saline infused air pouch tissue displayed very few inflammatory cells scattered within the tissue (Figure 7D). Thin wisps of collagen deposition were noted in the saline infused air pouch tissue (Figure 7J). Analysis of macrophage distribution in the 7-day saline infused tissue demonstrated that day 7 had a paucity of macrophages scattered in the air-pouch tissue (Figure 7P). Overall, the tissue reactions after 7-days of saline infusion (Figure 7D, J, P) were limited compared to the 3-day saline infused tissue reactions (Figure 7A, G, M).

Day 7 diluent infusion in diabetic mice: At 7-days post-diluent infusion, substantial amounts of inflammatory cells with enhanced cellularity were seen at the interface between the air pouch tissue and the air pouch (Figure 7E). Further analysis indicated a significant macrophages presence on day 7 (Figure 7Q). Additional collagen depositions were present at the 7-day diluent infusion site (Figure 7K). This collagen deposition was likely a result of expanded fibrosis at the air pouch tissue site.

Day 7 insulin infusion in diabetic mice: At 7-days of insulin (with diluent) infusion in diabetic mice, there was substantial inflammation at the air pouch tissue interface (Figure 7F). Additionally, inflammatory cells spread throughout the air pouch tissue (Figure 7F). Collagen deposition was seen at the tissue air pouch interface (Figure 7L). Macrophages were seen within the air pouch interface and the surrounding tissue, which was confirmed using F4/80 immunohistochemistry (Figure 7R).

In summary, the histopathologic evaluation of the air pouch tissue of both non-diabetic and diabetic mice demonstrated that saline infusion induced an acute tissue reaction characterized by limited inflammation. There was little to no collagen deposition, which abated by 7-days of saline infusion. In contrast, infusion of sterile diluent and diluent containing insulin infusions trigger more intense tissue reactions both at the air pouch interface and the adjoining air pouch tissue. These reactions included influx of neutrophils

and macrophages, particularly at the air pouch interface, and mild collagen deposition in both non-diabetic and diabetic mice.

Discussion

Current challenges to extending the lifespan of insulin infusion sets beyond its current 3-day FDA approval are limited by an incomplete understanding of the tissue reactions that contribute to this abbreviated lifespan (e.g. inflammation and wound healing). The underlying causes of CSII induced tissue reaction are likely multi-factorial. Cumulatively, the catheter material, shape, size, and the infused insulin formulation might contribute to the tissue reaction at the CSII infusion site. Other variables include the open wound and the catheter insertion angle, as investigated by Capillary Biomedical Inc. (Irvine, CA). Although several factors might induce inflammation at the infusion site, the specific mechanisms underlying CSII device failure have yet to be determined. Various hypotheses have been generated including mechanical barriers to insulin flow and direct toxicity from the infusion device's composition [12, 15, 16, 28]. However, this study focused on the root causes of the inflammatory response, specifically the phenolic compound used in insulin formulations, as well as the specific cell types responsible for the inflammation induced by these insulin phenolic compounds.

Cell toxicity of commercial insulins and diluents in vitro

All commercial insulin formulations contain phenol and m-cresol, which are classified as phenolic compounds due to their similarity in their chemical structure. Previous studies by Weber *et. al.*, demonstrated that commercial insulins containing phenolic compounds are toxic to a mouse cell line (L929) and a human cell line (THP-1) *in vitro* [11]. This investigation substantiated these findings and extended these studies to include mouse macrophages and fibroblast cell lines as these cells are key components in inflammation and wound healing. These studies demonstrated that commercial insulin formulations containing phenolic compounds are highly cytotoxic. When Zeba spin columns were utilized to remove cytotoxic phenolic compounds, (e.g. m-cresol and phenol), from standard insulin formulations, a minimal degree of cytotoxicity *in vitro* comparable to inert saline was observed. Specifically, these *in vitro* studies demonstrated that commercial insulins must be diluted at least 1:24 to minimize cytotoxicity in these cell populations.

Tissue toxicity of commercial insulin Humalog and phenolic compound, diluent

A mouse model was chosen for the initial *in vivo* studies designed to assess the role of specific leukocyte population involved in CSII at a molecular level. Given the plethora of deficient, knockout, and transgenic mice strains available, the mouse is uniquely able to parse the immunological mechanism underlying CSII variability in glycemic control. Nevertheless, this model has limitations given the differences between murine and human skin in that mice lack both apocrine sweat glands and rete ridges/dermal papillae. Rodent skin also presents a panniculus carnosus layer, which produces rapid contraction after injury, which differs from human wound healing that occurs by re-epithelialization and granulation tissue formation [29, 30]. These are all important differences to consider when evaluating infusion devices considered for human adipose-rich sites in mouse tissue. As such, future

studies should evaluate findings from the mouse model in a more pre-clinical animal model, such as the swine.

Although the mouse model is ideal for mechanistic inflammatory tests, the distribution of infused fluids into the loose mouse skin tissue, such as insulin including its phenolic compounds (e.g. sterile diluent), occurs in highly variable patterns due to tissue structure and gravity. This variable insulin/diluent flow complicates our ability to locate insulin flow pattern after an infusion. Thus, detecting insulin in tissue is difficult, which makes evaluation of insulin-induced tissue reactions challenging. As such, a predictable infusion site for histologic analysis is required to evaluate insulin and/or its diluent induced tissue reactions. The air pouch model has been extensively utilized for the evaluation of tissue responses to tissue irritants and/or for the evaluation of tissue reaction inhibitors [24, 25, 31–33]. We modified the classic murine air pouch model to investigate CSII causes and mechanisms associated with failures of maintaining euglycemia. One of the advantages of the air-pouch model is that it provides a defined compartment for the placement of solutions including insulins and related diluent *in vivo*. Using this mouse model, we demonstrated that insulin including diluent, and diluent-alone induces an infusion-site leukocytic influx in both control (non-diabetic) and STZ induced CD-1 diabetic mice.

Mouse *in vivo* studies demonstrated that sterile diluent could induce an inflammatory response in non-diabetic (control) mice as early as 3 days post-infusion. This response was still evident after 7 days when the study was terminated. Our data did not specifically address the duration of the inflammatory response beyond 7 days. Nonetheless, CSII infusion devices are not approved beyond 3 days of use. The same pattern was observed in chemically induced diabetic mice when saline was compared to diluent alone or diluted insulin. Thus, the mere presence of the insulin stabilizing phenolic compounds, such as sterile diluent, facilitates an inflammatory response. Mitigating this inflammatory response by neutralizing or eliminating these phenolic compounds is a promising means of extending CSII lifespan.

The leukocyte subpopulation FACS studies identified the specific cell types responsible for this inflammatory response. In the control mice, neutrophils were more prominent in the diluent infused group, but this did not reach statistical significance until day 7, whereas a reverse pattern was noted for lymphocytes in that they were more copious in the diluent group, but this only reached significance on day 3. Notably, monocytes and macrophages were more abundant in the diluent treated control mice on both days, although they were more numerous on day 3. This would be consistent with an acute inflammatory response, in which neutrophils and monocyte/macrophages are attracted to the injury site. Lymphocytes tend to be recruited early as noted here but persist only when there is an ongoing chronic inflammatory response [34]. Longitudinal studies were only conducted for a period of up to 7-days, which does not allow the necessary time frame to completely investigate chronic inflammation. Thus, our data supports the concept that phenolic compounds, such as diluent, may induce an inflammatory response even in the absence of diabetes.

These findings were further supported by noting that there were significantly greater numbers of leukocytes in the STZ-induced diabetic mice, irrespective of whether diluent

alone or diluent with insulin was infused. Moreover, there were no significant differences in the number of leukocytes on either day 3 or day 7, when comparing the diluent alone to the diluent with insulin in these mice. This indicates that the inflammatory response is dependent on the presence of diluent and not solely on the disease state.

The cellular subgroup analysis revealed significantly greater neutrophils on day 3 in the STZ-induced diabetic mice, when diluent was infused, as compared to the saline infused mice. While a similar trend was observed in the insulin treated mice, it did not reach statistical significance, as the study may have been under powered to detect this difference. This is supported by the concordant results of diluent and insulin throughout this experiment. This stands to reason, as diluted insulin tends to undergo 1:100 dilution for the mouse air pouch model, such that the remaining solution consists primarily of diluent. Due to the mouse size, the insulin Humalog with a phenolic compound concentration of 3.15 mg/ml (m-cresol) was diluted 1:100 using sterile diluent with a combined phenolic compound of 2.25 mg/ml. Given the 1:100 insulin dilution, the phenolic compounds in both insulin and sterile diluent alone are comparable when investigating mouse tissue reactions. This allows a direct correlation in the air pouch mouse model.

Figure 5A is remarkable as there was a trend in the STZ-induced diabetic mice in that both the diluent and insulin groups had more neutrophils than was observed in the saline group. This reached statistical significance during 3D infusion ($p<0.02$, Table 3C), but not after the 7D infusion (Table 3C). One plausible explanation is that there were insufficient numbers of mice in each of these groups such that the study was underpowered. Infusion of saline including the creation of an air pouch induces a mild inflammation, which is likely increased given the duration of the infusion study. This could also explain the increased numbers in neutrophils at day 7 of the infusion study. Nonetheless, these results demonstrate a robust inflammatory response as early as day 3, which implies that attenuating the neutrophilic response would result in less inflammation. A similar pattern was observed for monocyte/macrophage analysis. There were significantly greater numbers of these inflammatory cells in the insulin and diluent treated groups, as compared to the saline infused mice, whereas no differences were noted between the insulin and diluent treated groups. This indicates that the presence of phenolic compounds, such as diluent, induces a profound inflammatory response. With respect to the lymphocytes, a significant difference between these three states was detected at 3D, but not at 7D ($p<0.02$, Table 5C). Post-hoc analysis only demonstrated significantly fewer lymphocytes between the I and S groups at 3D ($p<0.02$, Table 5C). This further supports the hypothesis that diluent induces a profound acute inflammatory response. Thus, methodologies that would attenuate the inflammatory response could potentially extend the useful lifespan of CSII devices.

Histopathologic evaluation of air pouch walls

The histopathology of the air-pouch walls was qualitative, and not intended to be quantitative because of the confounding factor of the impact of the 10 ml lavage on the air pouch walls histopathology, which could create some artifacts in the air pouch wall tissue. That said, the qualitative histopathology analyses indicate that significantly less inflammation was observed in the saline treated air pouch tissue when compared to diluent

or insulin treated air pouch tissue. The similarities between diluent and diluted insulin-infused tissue reactivity is not remarkable given the concordance of these solutions. To avoid hypoglycemia, Humalog as the insulin of choice, is diluted in sterile diluent at a ratio of 1:100 in these studies. The H&E histology section demonstrated a diffuse red staining indicative of the presence of proteins (Figure 6 & 7). Thus, we opine that this protein layer at the air/tissue interface is likely the result from protein leaking from the vasculature as a consequence of increased vasopermeability occurring under inflammation including the accumulation of albumin, fibrinogen/fibrin and/or immunoglobulin. Tissue swelling from plasma influx was not observed in the air pouch model most likely due to the large size of the air pouch itself. Nevertheless, fluid influx is likely present due to vasopermability during inflammation. We did not observe significant differences between tissue reactions induced in non-diabetic animals versus STZ-induced diabetic animals when comparing infusion of reagents such as saline, diluent or diluted insulin. This may reflect the short duration of these studies as wound healing deficits observed with diabetes tend to reflect a chronic process. We also hypothesize that the increased tissue reactivity surrounding the diluent treated air pouch tissue is attributable to the phenolic compounds present in the sterile diluent solution. Furthermore, we opine that persistent acute inflammation during CSII alters infusion site tissue architecture and function. These studies also demonstrated that fibroblast recruitment and activation with resulting collagen deposition occurs at 3- and 7-days post-diluent and insulin infusion. The cumulative effect of this degree of fibrosis might limit the future utility of these infusion sites.

In summary, this study demonstrated that the mouse model is a cost-effective animal model that permits a detailed investigation on a molecular level into the sub-component processes regarding the inflammation associated with CSII. Future studies employing this model should be aimed at developing new approaches and therapeutics designed to prevent localized tissue reactions at the insulin infusion implantation sites. These data demonstrate that leukocytes, specifically neutrophils and monocytes/macrophages, sub-serve a critical role in the tissue reactions observed at the sites of subcutaneous insulin infusion. Thus, future research should be directed against the induced inflammatory response. Extended device functional lifespan has been achieved by attenuating inflammation through the incorporation of an anti-inflammatory agent, (e.g. dexamethasone), as reported by Senseonic [35]. Nevertheless, while non-specific anti-inflammatory agents extend the life expectancy of these diabetes management devices, they do not provide specific insights into the root causes of premature device failure. Once the precise mechanisms have been identified, precise inflammatory response inhibitors could be incorporated into the device coatings. Alternatively, the infusion set may be modified to contain more biocompatible materials as prior reports indicated that neither Teflon nor steel proved effective [14]. As sterile diluent was capable of inducing inflammation even in the absence of insulin, methods designed to reduce or neutralize these phenolic compounds' effects could extend device lifespan as well. Notwithstanding, it is imperative to attenuate the device associated inflammatory response in order to realize a functional artificial pancreas beyond its current 3-day lifespan.

Supplementary Material

Refer to Web version on PubMed Central for supplementary material.

Acknowledgements

We would like to thank Ms. Li Mao for her technical assistance. This work was supported by The Leona M. and Harry B. Helmsley Charitable Trust (2017PG-T1D008).

Abbreviations:

CSII	Continuous Subcutaneous Insulin Infusion
3D	3-days
7D	7-days
S	Saline
D	Diluent
I	Insulin
CD-1	Hsd:ICR
SD	Standard Deviation
BMMC	Bone Marrow-derived Mast Cells
PBMC	Peripheral Blood Mononuclear Cells
STZ	streptozotocin
CGM	Continuous Glucose Monitoring
H&E	Hematoxylin & Eosin

References

1. Rowley WR, et al. , Diabetes 2030: Insights from Yesterday, Today, and Future Trends. Popul Health Manag, 2017. 20(1): p. 6–12. [PubMed: 27124621]
2. U.S Food and Drug Administration. Freestyle Libre 14 Day Flash Glucose Monitoring System - P160030/S017 2018 [cited 2020 Aug 31st]; Available from: https://www.fda.gov/medical-devices/recently-approved-devices/freestyle-libre-14-day-flash-glucose-monitoring-system-p160030s017.
3. Pfutzner A, et al. , Using Insulin Infusion Sets in CSII for Longer Than the Recommended Usage Time Leads to a High Risk for Adverse Events: Results From a Prospective Randomized Crossover Study. J Diabetes Sci Technol, 2015. 9(6): p. 1292–8. [PubMed: 26341262]
4. Sampson Perrin AJ, et al. , A web-based study of the relationship of duration of insulin pump infusion set use and fasting blood glucose level in adults with type 1 diabetes. Diabetes Technol Ther, 2015. 17(5): p. 307–10. [PubMed: 25622214]
5. Thethi TK, et al. , Consequences of delayed pump infusion line change in patients with type 1 diabetes mellitus treated with continuous subcutaneous insulin infusion. J Diabetes Complications, 2010. 24(2): p. 73–8. [PubMed: 19395280]
6. Heinemann L and Krinelke L, Insulin infusion set: the Achilles heel of continuous subcutaneous insulin infusion. J Diabetes Sci Technol, 2012. 6(4): p. 954–64. [PubMed: 22920824]
7. Karlin AW, et al. , Duration of Infusion Set Survival in Lipohypertrophy Versus Nonlipohypertrophied Tissue in Patients with Type 1 Diabetes. Diabetes Technol Ther, 2016. 18(7): p. 429–35. [PubMed: 27227290]

8. Swan KL, et al. , Effect of age of infusion site and type of rapid-acting analog on pharmacodynamic parameters of insulin boluses in youth with type 1 diabetes receiving insulin pump therapy. Diabetes Care, 2009. 32(2): p. 240–4. [PubMed: 19017777]
9. Clausen TS, Kaastrup P, and Stallknecht B, Effect of insulin catheter wear-time on subcutaneous adipose tissue blood flow and insulin absorption in humans. Diabetes Technol Ther, 2009. 11(9): p. 575–80. [PubMed: 19764836]
10. Ponder SW, et al. , Unexplained hyperglycemia in continuous subcutaneous insulin infusion: evaluation and treatment. Diabetes Educ, 2008. 34(2): p. 327–33. [PubMed: 18375782]
11. Weber C, et al. , Phenolic excipients of insulin formulations induce cell death, pro-inflammatory signaling and MCP-1 release. Toxicology Reports, 2015. 2: p. 194–202. [PubMed: 28962351]
12. Hauzenberger JR, et al. , Detailed Analysis of Insulin Absorption Variability and the Tissue Response to Continuous Subcutaneous Insulin Infusion Catheter Implantation in Swine. Diabetes technology & therapeutics, 2017. 19(11): p. 641–650. [PubMed: 28981324]
13. Renard E and Boizel R, Comments on Patel et al.'s "Randomized trial of infusion set function: steel versus teflon": early catheter failures may differ according to teflon catheter model. Diabetes Technol Ther, 2014. 16(8): p. 545–6. [PubMed: 24967507]
14. Patel PJ, et al. , Randomized trial of infusion set function: steel versus teflon. Diabetes Technol Ther, 2014. 16(1): p. 15–9. [PubMed: 24090124]
15. Hauzenberger JR, et al. , Author Correction: Systematic in vivo evaluation of the time-dependent inflammatory response to steel and Teflon insulin infusion catheters. Scientific reports, 2019. 9(1): p. 6183–6183. [PubMed: 30971716]
16. Hauzenberger JR, et al. , Systematic in vivo evaluation of the time-dependent inflammatory response to steel and Teflon insulin infusion catheters. Sci Rep, 2018. 8(1): p. 1132. [PubMed: 29348570]
17. Duan W, et al. , Ecotoxicity of phenol and cresols to aquatic organisms: A review. Ecotoxicol Environ Saf, 2018. 157: p. 441–456. [PubMed: 29655160]
18. World Health Organization. Cresols : health and safety guide 1996 [cited 2020 Aug 31st]; Available from: https://apps.who.int/iris/handle/10665/38142?search-result=true&query=cresols&scope=&rpp=10&sort_by=score&order=desc.
19. Bode BW, Comparison of pharmacokinetic properties, physicochemical stability, and pump compatibility of 3 rapid-acting insulin analogues-aspart, lispro, and glulisine. Endocr Pract, 2011. 17(2): p. 271–80. [PubMed: 21134878]
20. Renard E, et al. , Lower rate of initial failures and reduced occurrence of adverse events with a new catheter model for continuous subcutaneous insulin infusion: prospective, two-period, observational, multicenter study. Diabetes Technol Ther, 2010. 12(10): p. 769–73. [PubMed: 20809682]
21. Klueh U, et al. , Critical role of tissue mast cells in controlling long-term glucose sensor function in vivo. Biomaterials, 2010. 31(16): p. 4540–51. [PubMed: 20226521]
22. Woods RJ, et al. , Intrinsic fibrillation of fast-acting insulin analogs. J Diabetes Sci Technol, 2012. 6(2): p. 265–76. [PubMed: 22538135]
23. Wu KK and Huan Y, Streptozotocin-induced diabetic models in mice and rats. Curr Protoc Pharmacol, 2008. Chapter 5: p. Unit 5 47.
24. Dawson J, et al. , A comparative study of the cellular, exudative and histological responses to carrageenan, dextran and zymosan in the mouse. Int J Tissue React, 1991. 13(4): p. 171–85. [PubMed: 1726538]
25. Duarte DB, Vasko MR, and Fehrenbacher JC, Models of inflammation: carrageenan air pouch. Curr Protoc Pharmacol, 2012. Chapter 5: p. Unit5 6.
26. Magilavy DB, Animal models of chronic inflammatory arthritis. Clin Orthop Relat Res, 1990(259): p. 38–45.
27. Unsworth A, et al. , OMIP-032: Two multi-color immunophenotyping panels for assessing the innate and adaptive immune cells in the mouse mammary gland. Cytometry A, 2016. 89(6): p. 527–30. [PubMed: 27214375]

28. Eisler G, et al. , In vivo investigation of the tissue response to commercial Teflon insulin infusion sets in large swine for 14 days: the effect of angle of insertion on tissue histology and insulin spread within the subcutaneous tissue. BMJ Open Diabetes Res Care, 2019. 7(1): p. e000881.
29. Rodrigues M, et al. , Wound Healing: A Cellular Perspective. Physiol Rev, 2019. 99(1): p. 665–706. [PubMed: 30475656]
30. Eming SA, Martin P, and Tomic-Canic M, Wound repair and regeneration: mechanisms, signaling, and translation. Sci Transl Med, 2014. 6(265): p. 265sr6. [PubMed: 25473038]
31. El-Achkar GA, et al. , Heme oxygenase-1-Dependent anti-inflammatory effects of atorvastatin in zymosan-injected subcutaneous air pouch in mice. PLoS One, 2019. 14(5): p. e0216405. [PubMed: 31071151]
32. Ulleryd MA, et al. , Stimulation of alpha 7 nicotinic acetylcholine receptor (alpha7nAChR) inhibits atherosclerosis via immunomodulatory effects on myeloid cells. Atherosclerosis, 2019. 287: p. 122–133. [PubMed: 31260875]
33. Wei R, Wu J, and Li Y, Macrophage polarization following three-dimensional porous PEEK. Mater Sci Eng C Mater Biol Appl, 2019. 104: p. 109948. [PubMed: 31499957]
34. Moro-Garcia MA, et al. , Influence of Inflammation in the Process of T Lymphocyte Differentiation: Proliferative, Metabolic, and Oxidative Changes. Front Immunol, 2018. 9: p. 339. [PubMed: 29545794]
35. Aronson R, Abitbol A, and Tweden KS, First assessment of the performance of an implantable continuous glucose monitoring system through 180 days in a primarily adolescent population with type 1 diabetes. Diabetes Obes Metab, 2019. 21(7): p. 1689–1694. [PubMed: 30938036]

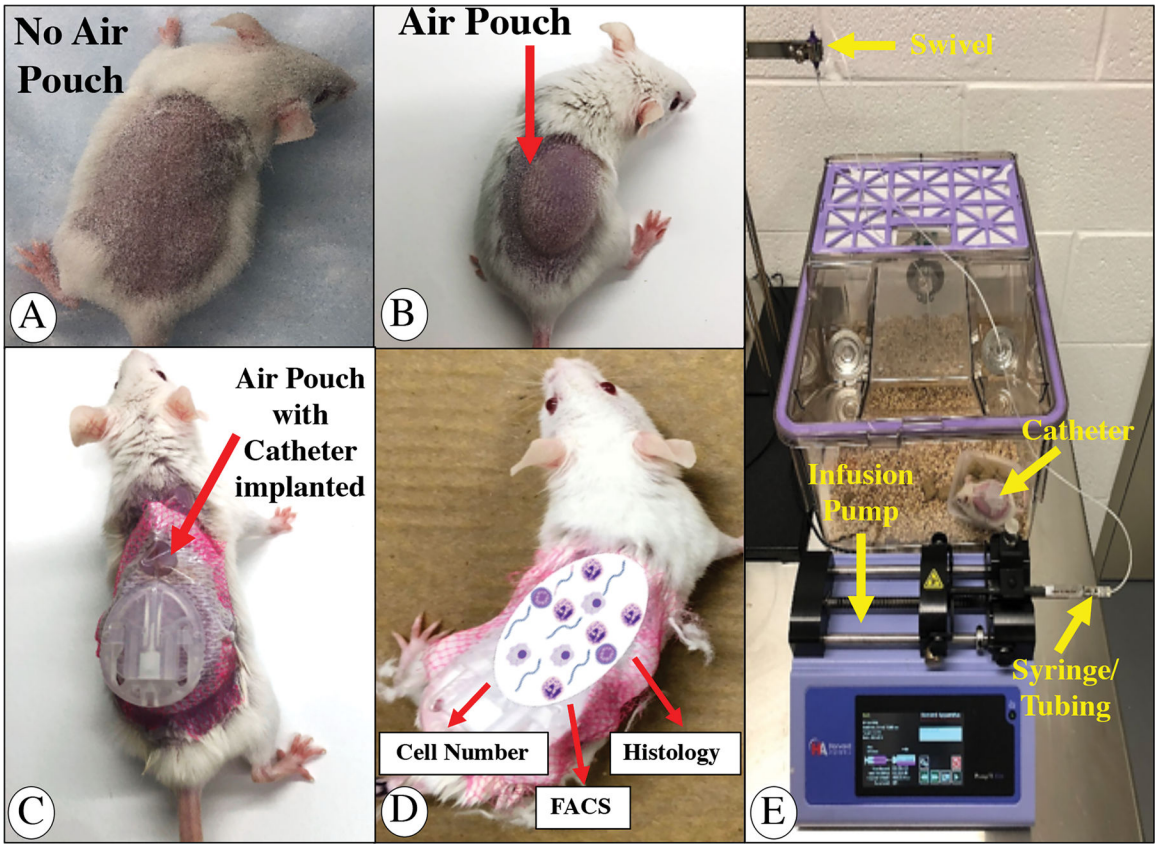

Figure 1. Murine air pouch model for infusion studies

Shaved mouse back prior to air pouch formation (A), post air pouch formation (B) including pediatric catheter implantation into air pouch (C). (D) summarizes the air pouch analyses and (E) is a picture of the murine infusion set up.

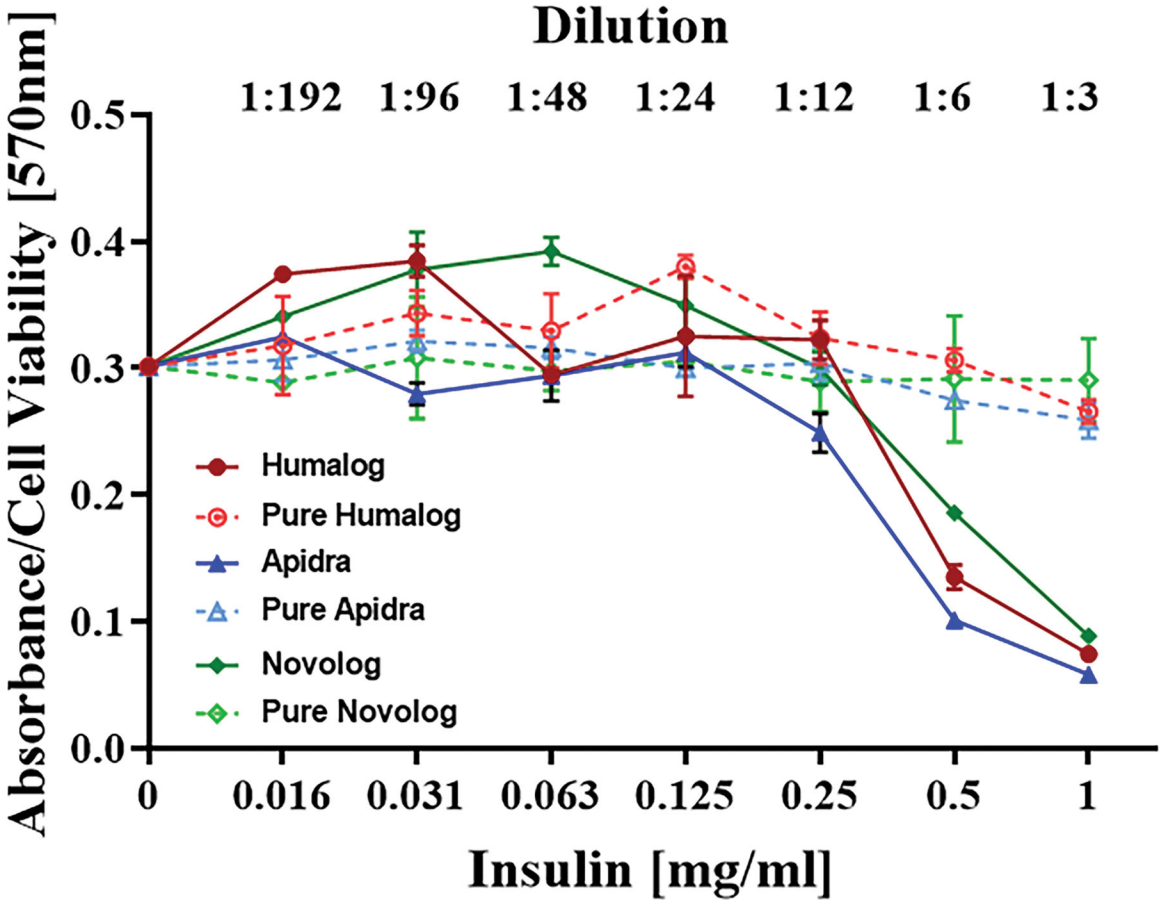

Figure 2. Concentration-dependent insulin toxicity on human PBMCs *in vitro*

PBMCs were exposed to Humalog, Apidra, and Novolog in a dose dependent manner (0–1 mg/mL) for 1-day. Cells were exposed to these commercial insulin formulations with and without added phenolic compounds. MTT assay was used to analyze cell viability, and absorbance was read at 570 nm. Error bars indicate standard deviation.

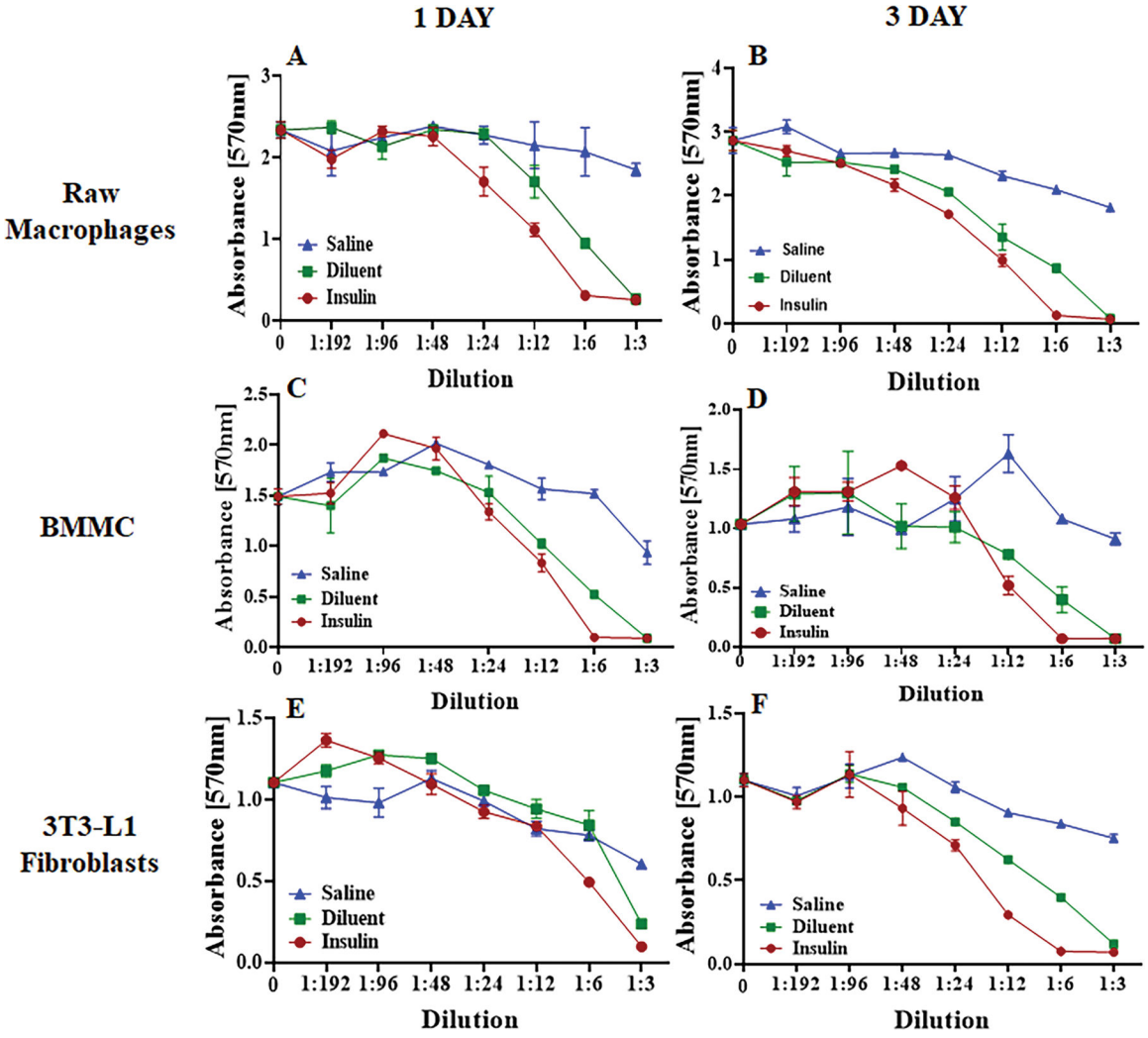

Figure 3. Cytotoxicity of Humalog and diluent on mouse cell lines *in vitro*

A-B) Raw macrophages, C-D) BMMC (Bone Marrow-derived Mast Cells), and E-F) 3T3-L1 fibroblasts were exposed to saline, diluent (phenolic compounds), and insulin (Humalog) for 1- and 3-days at different concentrations. Cell toxicity was measured using an MTT assay and absorbance was read at 570nm. Error bars indicate standard deviation.

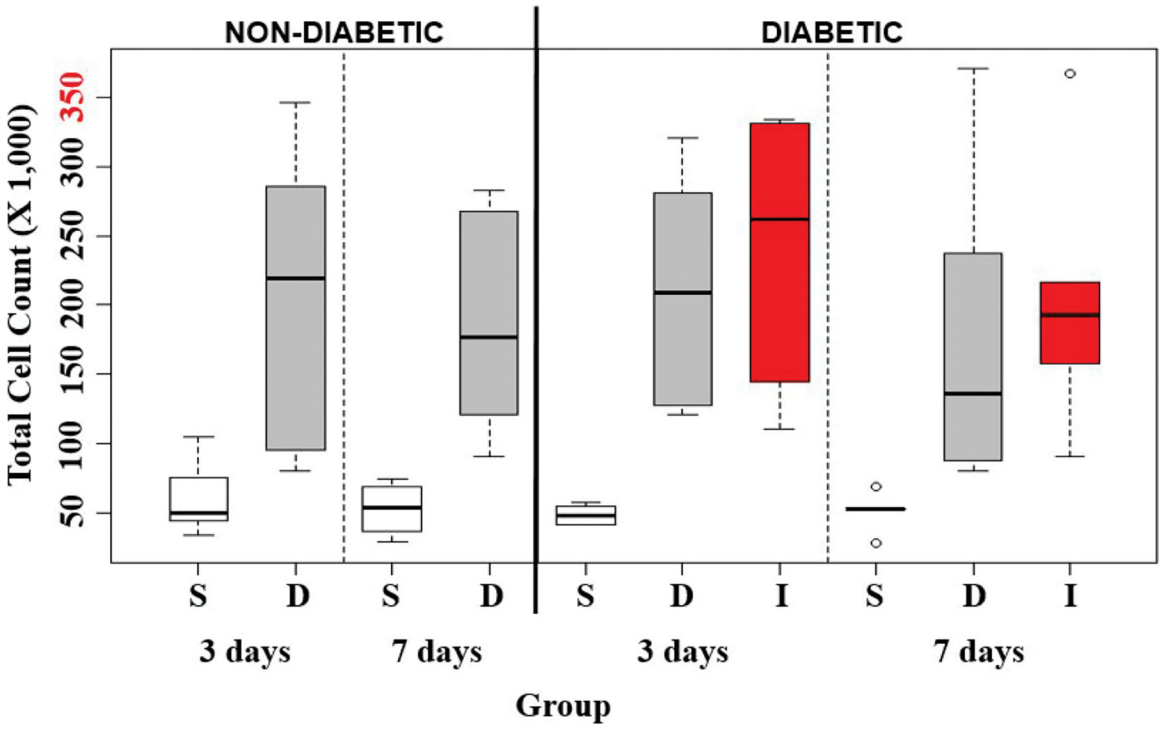

Figure 4. Quantification of total leukocytes

Total leukocytes harvested following the infusion of saline (S), diluent (D), and insulin (I) into the air pouch of non-diabetic and STZ-induced diabetic CD-1 mice for 3-days and 7-days using FACS analysis. Small circles represent outliers and were not included in statistical analyses. Red labeled number on y-axis is the maximum number of leukocytes collected.

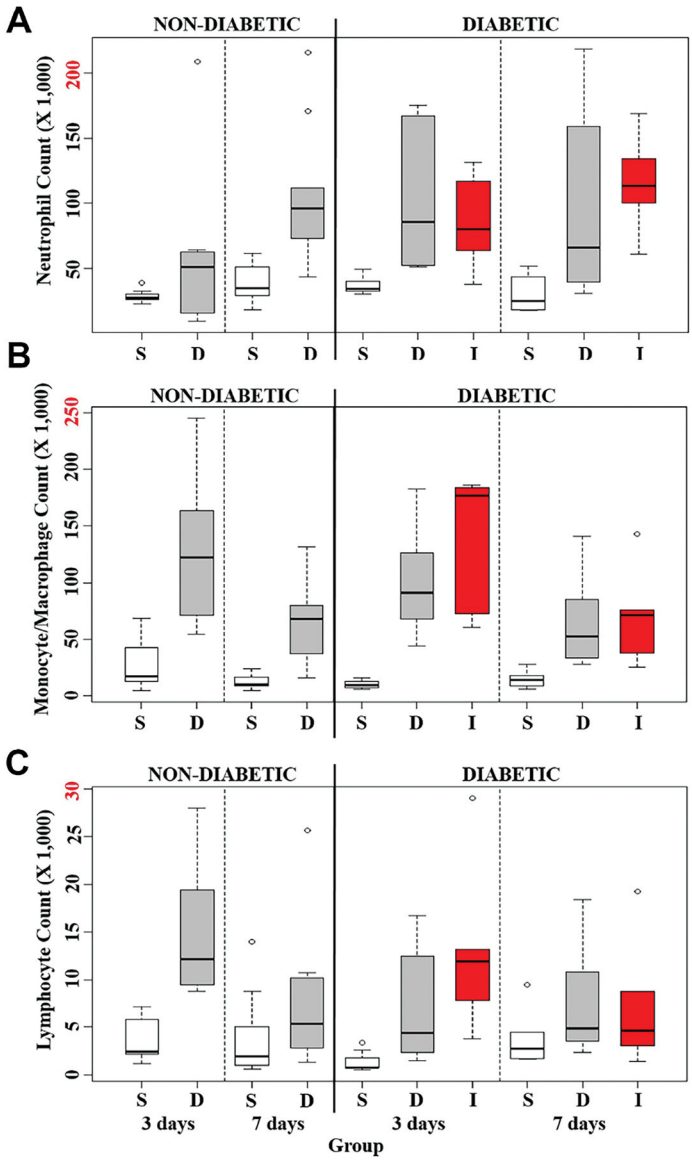

Figure 5. Quantification of leukocyte cell types

Total leukocyte cell types harvested from the infusion of saline (S), diluent (D), and insulin (I) into the air pouch of normal and STZ-induced diabetic CD-1 mice. The total A) Neutrophils, B) Macrophages/Monocytes, and C) Lymphocytes collected from the air pouch cell exudate were quantified using FACS analysis. Small circles represent outliers and were not included in statistical analyses. Red labeled number on y-axis is the maximum number of leukocytes collected for each respective cell population.

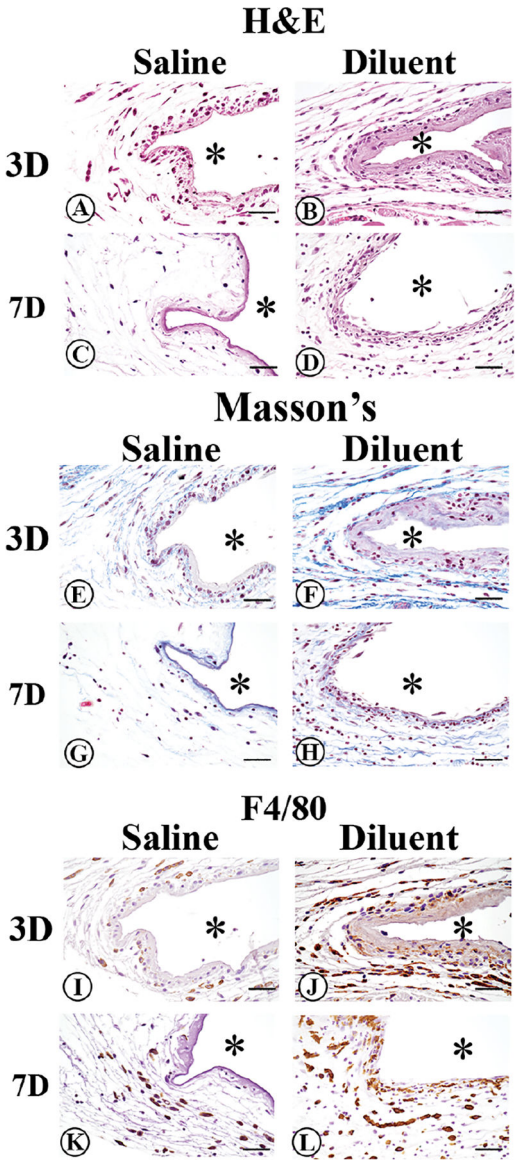

Figure 6. Histopathologic evaluation of the tissue reaction induced in non-diabetic CD-1 mice following saline or diluent infusion

To evaluate tissue reactions at site of diluent (phenolic compounds) or saline infusion, mouse air pouch tissue was obtained at 3- or 7-days post-infusion. Standard hematoxylin and eosin (H&E) stain (Figure 6A–D), Masson's Trichrome stain (Figure 6E–H), and immunohistochemical staining of macrophages using the macrophage-specific F4/80 antibody (Figure 6I–L) was employed. Original air pouch location is depicted by (*), magnification is at 40x, and scalebar is 10μm.

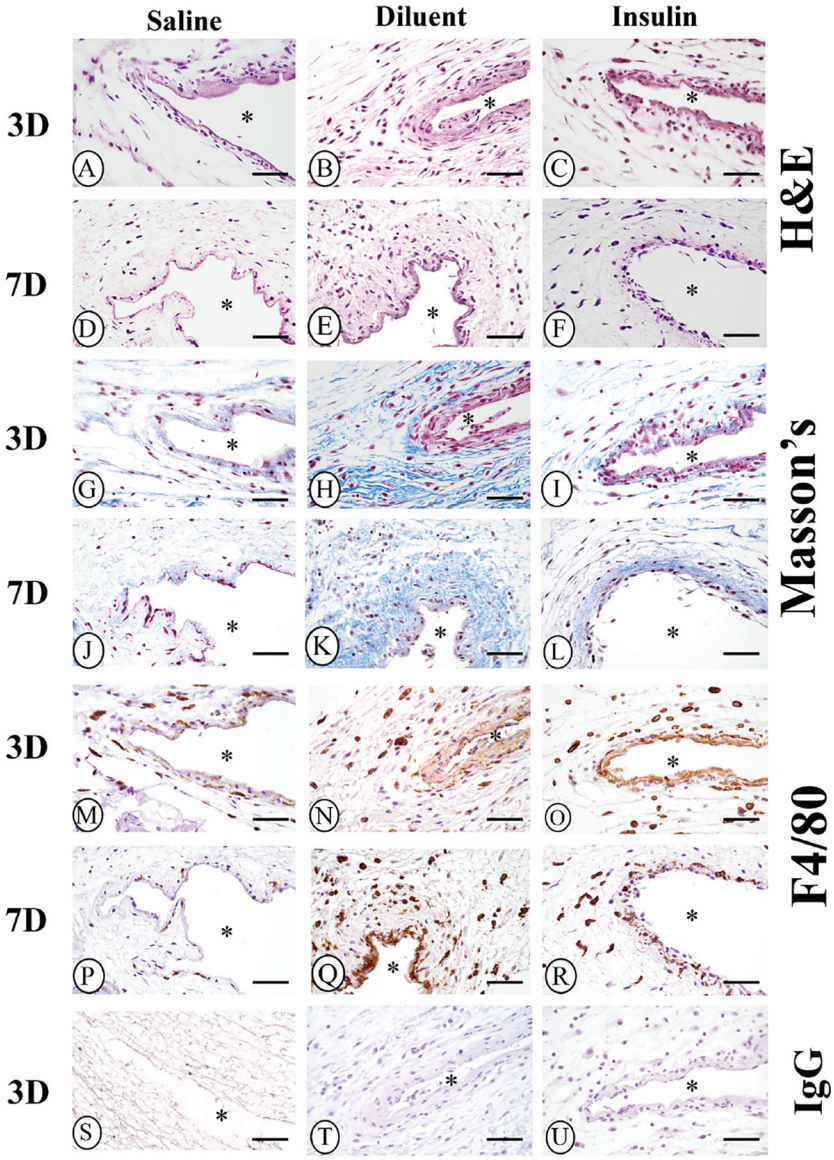

Figure 7. Qualitative histopathologic evaluation of the tissue reaction in STZ-induced diabetic CD-1 mice following saline, diluent, or insulin infusion

Histopathologic analysis of air pouch tissue following 3- and 7-day infusion of saline, diluent (phenolic compounds), and diluted insulin was performed using standard Hematoxylin and Eosin (H&E) stain (Figure 7A–F), and Masson's Trichrome stain (Figure 7G–L). Immunohistochemistry analysis of macrophage presence and distribution was performed using a macrophage-specific F4/80 antibody (Figure 7M–R). Controls of normal IgG are depicted in Figure 7S–U. Original air pouch location is depicted by (*), magnification is at 40x, and scalebar is 10μm.

Table 1.

Fast-acting insulin formulations used in continuous subcutaneous insulin infusion (CSII).

Brand Name	Generic Name	Meta Cresol (mg/mL)	Phenol (mg/mL)	Manufacturer	Concentration of Insulin in 100U (mg/mL)	Other Ingredients
Apidra	**Insulin Glulisine**	**3.15**	**N/A**	**Sanofi-Aventis**	**3.49**	Tromethamine (6 mg/mL), Sodium Chloride (5 mg/mL) Sodium Chloride (0.01 mg/mL)
Fiasp	**Aspart**	**1.72**	**1.5**	**Novo Nordisk**	**3.5**	Zinc acetate (19.6 mcg), Disodium phosphate dihydrate (0.53 mg), Arginine hydrochloride (3.48 mg), Nicotinamide (vitamin B3) (20.8 mg), Hydrochloric acid (for pH adjustment), Sodium hydroxide (for pH adjustment), Water for injections
HumalogU-100	**InsulinLispro**	**3.15**	**Trace amounts**	**Eli Lilly**	**3.47**	Zinc (19.7μg/mL), Dibasic Sodium Phosphate (1.88 mg/mL), Glycerin (16 mg/mL)
NovoLog*known as Novorapid in Europe	**Aspart**	**1.72**	**1.5**	**Novo Nordisk**	**3.47**	Zinc (19.6 μg/mL), Disodium Hydrogen Phosphatedihydrate (1.25 mg/mL), Glycerin (16 mg/mL), Sodium Chloride (0.58 mg/mL)
Insuman Infusat*only available in Europe	**Insulin Human**	**N/A**	**2.7**	**Sanofi-Aventis**	**3.5**	Zinc chloride(0.058mg/mL), Trometamol (6mg/mL) Glycerol (20mg/mL), Poly(oxyethylene, oxypropylene) glycol (0.01 mg/mL), Hydrochloric acid (3.7 mg/mL)
SterileDiluent	**Diluent**	**1.6**	**0.65**	**Eli Lilly**	**N/A**	Glycerin (16mg/mL), Sodium Phosphate Dibasic (3.8 mg/mL), Water for Injections, q.s, Hydrochloric Acid and/or Sodium Hydroxide may have been added to adjust pH

Sterile Diluent, not an insulin formulation, is highlighted in grey. This is included in the table in order to be comprehensive as it was used throughout the studies.

Table 2.

Statistical Analysis of Total Cells data from Mouse Air Pouch Model

A. Raw Data: Total Cells

Total Cell (x1,000)							
Mouse Status		**3D**			**7D**		
		N	**Mean**	**SD**	**N**	**Mean**	**SD**
Non-diabetic	S	8	60	27	14	54	16
	D	8	204	105	10	182	74
Diabetic	S	7	49	7	5	51	14
	I	5	237	104	5	205	102
	D	6	212	87	8	172	102

B. S vs. D

P value from two-sample t-tests		
Non-Diabetic	3D	<0.01
Non-Diabetic	7D	<0.001

C. S vs. D vs. I

P value from one-way ANOVA and Tukey post-hoc adjustment					
		S vs. D. vs. I	**D vs. I**	**I vs. S**	**D vs. S**
Diabetic	3D	<0.001	NS	<0.01	<0.01
Diabetic	7D	<0.05	NS	<0.05	NS

D. 3D vs. 7D

P value from two-sample t-tests		
Non-Diabetic	S	NS
Non-Diabetic	D	NS
Diabetic	S	NS
Diabetic	D	NS
Diabetic	I	NS

E. Non-diabetic vs. Diabetic

P value from two-sample t-tests		
S	3D	NS
S	7D	NS
D	3D	NS
D	7D	NS

A) Data represents n-value, mean, and standard deviation (SD) for total leukocyte recruitment following infusion of saline (S), diluent (D), and insulin (I) for 3-days (3D) and 7-days (7D) in non-diabetic and diabetic mice;

B) p-values for infusion of S versus D for 3D and 7D in non-diabetic animals;

C) p-values for infusion of S, D, and I for 3D and 7D in diabetic animals;

D) p-values for 3D versus 7D infusion of S, D, I in non-diabetic and diabetic animals;

E) p-values for non-diabetic versus diabetic infusion of S and D for 3D and 7D.

Table 3.

Statistical Analysis of Neutrophils data from Mouse Air Pouch Model

A. Raw Data: Neutrophils

Total Cell (x1,000)

Mouse Status		3D			7D		
		N	Mean	SD	N	Mean	SD
Non-diabetic	S	8	29	5	14	38	14
	D	8	60	64	10	106	52
Diabetic	S	7	37	7	5	31	16
	I	5	86	38	5	116	40
	D	6	103	56	8	97	75

B. S vs. D

P value from two-sample t-tests

Non-Diabetic	3D	NS
Non-Diabetic	7D	<0.01

C. S vs. D vs. I

P value from one-way ANOVA and Tukey post-hoc adjustment

		S vs. D. vs. I	D vs. I	I vs. S	D vs. S
Diabetic	3D	<0.02	NS	NS	<0.02
Diabetic	7D	NS	NS	NS	NS

D. 3D vs. 7D

P value from two-sample t-tests

Non-Diabetic	S	<0.05
Non-Diabetic	D	NS
Diabetic	S	NS
Diabetic	D	NS
Diabetic	I	NS

E. Non-diabetic vs. Diabetic

P value from two-sample t-tests

S	3D	<0.02
S	7D	NS
D	3D	NS
D	7D	NS

A) Data represents n-value, mean, and standard deviation (SD) for total Neutrophil recruitment following infusion of saline (S), diluent (D), and insulin (I) for 3-days (3D) and 7-days (7D) in non-diabetic and diabetic mice;

B) p-values for infusion of S versus D for 3D and 7D in non-diabetic animals;

C) p-values for infusion of S, D, and I for 3D and 7D in diabetic animals;

D) p-values for 3D versus 7D infusion of S, D, I in non-diabetic and diabetic animals;

E) p-values for non-diabetic versus diabetic infusion of S and D for 3D and 7D.

Table 4.

Statistical Analysis for Macrophage/Monocyte data from Mouse Air Pouch Model

A. Raw Data: Macrophages/Monocytes

Total Cell (x1,000)

Mouse Status		3D			7D		
		N	Mean	SD	N	Mean	SD
Non-diabetic	S	8	27	24	14	12	6
	D	8	127	66	10	64	34
Diabetic	S	7	10	4	5	15	9
	I	5	136	64	5	71	46
	D	6	100	49	8	64	40

B. S vs. D

P value from two-sample t-tests

Non-Diabetic	3D	<0.01
Non-Diabetic	7D	<0.001

C. S vs. D vs. I

P value from one-way ANOVA and Tukey post-hoc adjustment

		S vs. D. vs. I	D vs. I	I vs. S	D vs. S
Diabetic	3D	<0.001	NS	<0.001	<0.01
Diabetic	7D	<0.05	NS	NS	NS

D. 3D vs. 7D

P value from two-sample t-tests

Non-Diabetic	S	NS
Non-Diabetic	D	<0.02
Diabetic	S	NS
Diabetic	D	NS
Diabetic	I	NS

E. Non-diabetic vs. Diabetic

P value from two-sample t-tests

S	3D	NS
S	7D	NS
D	3D	NS
D	7D	NS

A) Data represents n-value, mean, and standard deviation (SD) for total Macrophage/Monocyte recruitment following infusion of saline (S), diluent (D), and insulin (I) for 3-days (3D) and 7-days (7D) in non-diabetic and diabetic mice;

B) p-values for infusion of S versus D for 3D and 7D in non-diabetic animals;

C) p-values for infusion of S, D, and I for 3D and 7D in diabetic animals;

D) p-values for 3D versus 7D infusion of S, D, I in non-diabetic and diabetic animals;

E) p-values for non-diabetic versus diabetic infusion of S and D for 3D and 7D.

Table 5.

Statistical Analysis for Lymphocyte data from Mouse Air Pouch Model

A. Raw Data: Lymphocytes

		Total Cell (x1,000)					
Mouse Status		**3D**			**7D**		
		N	**Mean**	**SD**	**N**	**Mean**	**SD**
Non-diabetic	S	8	4	2	14	4	4
	D	8	15	7	10	7	7
Diabetic	S	6	7	6	8	7	6
	I	5	13	10	5	7	7
	D	6	7	6	8	7	6

B. S vs. D

P value from two-sample t-tests		
Non-Diabetic	3D	<0.01
Non-Diabetic	7D	NS

C. S vs. D vs. I

P value from one-way ANOVA and Tukey post-hoc adjustment					
		S vs. D. vs. I	**D vs. I**	**I vs. S**	**D vs. S**
Diabetic	3D	<0.02	NS	<0.02	NS
Diabetic	7D	NS	NS	NS	NS

D. 3D vs. 7D

P value from two-sample t-tests		
Non-Diabetic	S	NS
Non-Diabetic	D	NS
Diabetic	S	NS
Diabetic	D	NS
Diabetic	I	NS

E. Non-diabetic vs. Diabetic

P value from two-sample t-tests		
S	3D	<0.05
S	7D	NS
D	3D	NS
D	7D	NS

A) Data represents n-value, mean, and standard deviation (SD) for total lymphocyte recruitment following infusion of saline (S), diluent (D), and insulin (I) for 3-days (3D) and 7-days (7D) in non-diabetic and diabetic mice;

B) p-values for infusion of S versus D for 3D and 7D in non-diabetic animals;

C) p-values for infusion of S, D, and I for 3D and 7D in diabetic animals;

D) p-values for 3D versus 7D infusion of S, D, I in non-diabetic and diabetic animals;

E) p-values for non-diabetic versus diabetic infusion of S and D for 3D and 7D.